Aharonov-Bohm scattering of wave packets by Maxwell coils

M. Jursa and P. Kasperkovitz
Institut für Theoretische Physik, Technische Universität Wien, Wiedner Hauptstraße 8-10, A-1040 Wien, Austria
(Received 25 November 1992)

Maxwell coils are solenoids of spheroidal shape which produce a constant magnetic field inside the coil; at large distances the field of a Maxwell coil becomes that of a magnetic dipole. The current in systems consisting of several confocal Maxwell coils can be adjusted in such a way that the magnetic field inside the smallest coil is constant and the back flux is confined to the interior of the largest coil. Quantum-mechanical scattering of charged particles by Maxwell coils, or systems thereof, is first formulated as a three-dimensional problem and then treated within a two-dimensional approximation. The evolution in time of wave packets, which are Gaussian wave packets in the beginning, is calculated numerically. In all cases an Aharonov-Bohm effect is observed in the angular distribution of the scattered wave packets. The back flux results only in an additional deflection of the packets, which corresponds to the classical deflection caused by the Lorentz force.

PACS number(s): 03.65.Bz, 03.65.Nk

I. INTRODUCTION

In 1959 Aharonov and Bohm (AB) [1] pointed out that electromagnetic potentials can influence the quantum-mechanical motion of charged particles even in regions where the fields derived from the potentials vanish. This assertion gave rise to a long and often passionate discussion on the existence and meaning of this effect, including the interpretation of experiments that were performed to verify AB's proposition. A fair survey of this controversy is given by Tonomura in [2]; for additional information see the survey article by Olariu and Popescu [3]. Although the majority of physicists now seems to believe in the existence of the AB effect, the theoretical description of many (actual or thought) experiments still contains a number of ad hoc assumptions and simplifications which call for a more detailed analysis.

In order to illustrate their general ideas Aharonov and Bohm [1] calculated the differential cross section for electrons scattered by an inpenetrable solenoid (magnetic AB effect). The solenoid was assumed to have the form of an ideal cylinder of infinite length so that the magnetic field is completely trapped inside the coil. (In addition, the radius of the coil was assumed to be vanishingly small, but this assumption was only made to simplify the calculations and is irrelevant for the following). As an infinite solenoid cannot be realized experimentally, a number of authors [4] considered the question whether the magnetic field, which exists outside of every finite coil, might be responsible for the magnetic AB effect. A scattering problem with closed magnetic flux was considered by Peshkin *et al.* [5], who studied for a pair of two parallel infinite solenoids, which carry opposite currents, the form of the wave function in the plane joining the two cylinders; afterwards Tassie [6] extended these arguments to a toroidal coil. A more detailed analysis of these problem was given later by Olariu and Popescu [3]. All these authors conclude that the magnetic AB effect, i.e., the dependence of the interference pattern behind the coil(s) on the magnetic flux in the inaccessible region(s), exists also for closed magnetic fluxes. Whereas the space accessible to the electrons is free of fields in these models, the current distribution considered by Liang [7] and Kobe and Liang [8] yields a nonvanishing magnetic field not only inside the shielded solenoid but also in an infinitely thin cylindrical shell that encloses this coil and serves to close the magnetic flux. As the AB cross section is approached when the radius of the shell tends to infinity these authors conclude that the AB effect may be attributed to the Lorentz force of the return flux. Kobe [9] also discussed the combined effect of magnetic field and shieded flux in the two-slit diffraction experiment and found both AB interference and a shift of the diffraction pattern due to the Lorentz force. We finally mention the work of Babiker and Loudon [10] who considered a solenoid of finite length and calculated the enclosed flux responsible for the AB phase shift for closed paths consisting of semicircular or straight segments. Apart from the fact that the magnetic field was only calculated within an approximation, the main difference to the work of Kobe and Liang is that the interactions, which cause the splitting of the incoming beam in front of the coil and unite the two parts behind it, are not included in the analysis of Babiker and Loudon (in the other models beam splitting was effected by the hard-core potential of the shield).

In this paper the scattering problem of AB and its modification by Liang and Kobe are reconsidered. Instead of the infinite cylindrical solenoids used in [1, 7, 8] we consider solenoids of prolate spheroidal shape which produce a constant field inside and a nonvanishing field outside the coil. The properties of such a solenoid, often called a Maxwell coil in the literature, are reviewed in Sec. II, where we also consider systems consisting of two and three confocal coils. Assuming the central coil to be impenetrable we then formulate the three-dimensional scattering problem in Sec. III and discuss its classical so-

lutions. From the study of these classical orbits we conclude that the three-dimensional problem may be approximated by a two-dimensional one if (i) the coil is sufficiently long, (ii) the time interval in which the evolution is followed is bounded, and (iii) during this period the particle moves within a thin planar sheet normal to the coil's axis. In Sec. IV the corresponding two-dimensional scattering problem is considered. It differs from similar discussions in the literature by the existence of spatially extended magnetic field(s) outside the shielded flux, and by considering time-dependent wave functions instead of stationary ones. The advantage of a time-dependent approach is that use of square-integrable wave functions automatically eliminates apparent paradoxa, such as the diverging cross sections which are obtained in a time-independent treatment of AB scattering [11]. For vanishing magnetic fields AB scattering of wave packets has been studied previously by analytical methods [12, 3]. In Sec. IV of this paper the time-dependent Schrödinger equation is solved numerically, the initial data representing the free motion of a Gaussian wave packet. Snapshots of wave packets at different instants are presented for one and more coils, both of finite and of infinite length. Among the examples studied in detail is the string-plus-shield model of Liang and Kobe [7, 8] whose conclusions are critically analyzed. Finally, in Sec. V we summarize the general features of AB scattering as they emerge from the examples studied in Sec. IV.

II. MAXWELL COILS

Prolate spheroidal coordinates (ξ, η, φ) are related to Cartesian coordinates (x, y, z) by [13]

$$\begin{aligned} r_\pm &= \sqrt{x^2 + y^2 + (z \pm \epsilon)^2}, \\ \xi &= (r_+ + r_-)/2\epsilon, \\ \eta &= (r_+ - r_-)/2\epsilon, \\ \varphi &= \arctan(x/y), \end{aligned} \tag{1}$$

the range of the variables being $1 \le \xi < \infty$, $-1 \le \eta \le 1$, $0 \le \varphi \le 2\pi$. The surfaces $\xi = \xi_1 = \text{const}$ are prolate spheroids (foci at $\pm\epsilon$, height $2L_1 = 2\epsilon\xi_1$, maximal diameter $2R_1 = 2\epsilon\sqrt{\xi_1^2 - 1}$). If a wire of constant cross section is densely wound around such a spheroid such that the loops are normal to its axis, one obtains a Maxwell coil. For thin wires the current in such a coil may be considered as surface current.

$$\mathbf{j}(\xi, \eta, \varphi) = J_1 \, \frac{\sqrt{1 - \eta^2}}{\xi_1^2 - \eta^2} \, \delta(\xi - \xi_1) \, \mathbf{n}_\varphi . \tag{2}$$

The corresponding solution of the vector Laplace equation, which is transversal and satisfies natural boundary conditions, is [13, 14]

$$\mathbf{A}(\xi, \eta, \varphi) = A_1 \times \left\{ \begin{matrix} Q_1^1(\xi_1) P_1^1(\xi) \\ P_1^1(\xi_1) Q_1^1(\xi) \end{matrix} \right\} \times \sqrt{1 - \eta^2} \, \mathbf{n}_\varphi , \tag{3}$$

where the upper line holds for $\xi < \xi_1$ and the lower one for $\xi > \xi_1$; the functions P_l^m and Q_l^m are the associated Legendre functions of the first and second kind [14, 15], respectively.

$$\left. \begin{matrix} P_1^1(\xi) \\ Q_1^1(\xi) \end{matrix} \right\} = \sqrt{\xi^2 - 1} \, \frac{\partial}{\partial \xi} \left\{ \begin{matrix} P_1^0(\xi) \\ Q_1^0(\xi) \end{matrix} \right. , \tag{4}$$

$$P_1^0(\xi) = \xi, \quad Q_1^0(\xi) = \frac{\xi}{2} \ln\left(\frac{\xi + 1}{\xi - 1} \right) - 1. \tag{5}$$

The magnetic field obtained from the vector potential (3) is constant inside the coil $(\xi < \xi_1)$,

$$\mathbf{B}(\xi, \eta, \varphi) = B_1 \, \mathbf{n}_z , \tag{6}$$

whereas in the exterior $(\xi > \xi_1)$ it is given by

$$\begin{aligned} B_\xi(\xi, \eta, \varphi) &= -B_1' \, Q_1^1(\xi) \, \eta / \sqrt{\xi^2 - \eta^2}, \\ B_\eta(\xi, \eta, \varphi) &= -B_1' \, Q_1^0(\xi) \, \sqrt{1 - \eta^2} / \sqrt{\xi^2 - \eta^2}, \\ B_\varphi(\xi, \eta, \varphi) &= 0 . \end{aligned} \tag{7}$$

The relation between the constants J_1, A_1, B_1, and B_1' is

$$\begin{aligned} A_1 &= 2\pi\epsilon^2 \, J_1/c, \\ B_1 &= 4\pi\epsilon Q_1^1(\xi_1) \, J_1/c, \\ B_1' &= 4\pi\epsilon\sqrt{\xi_1^2 - 1} \, J_1/c . \end{aligned} \tag{8}$$

A Maxwell coil is therefore uniquely determined by two geometrical parameters, say ϵ and R_1, and the flux parameter

$$\alpha = B_1 R_1^2/2 \tag{9}$$

(the total flux through the plane $z = 0$ is, of course, equal to zero).

At large distances from the coil $(r = \sqrt{x^2 + y^2 + z^2} \gg \epsilon)$ the field (7) becomes that of a magnetic dipole ($\xi \approx r/\epsilon$, $\eta \approx \cos\vartheta$, $A_\xi \approx A_r = 2M\cos\vartheta/r^2$, $A_\eta \approx -A_\vartheta = -M\sin\vartheta/r^2$, $M = -B_1'\epsilon^3/3$). On the other hand, if the coil is slim ($\epsilon \gg R_1$) and the field is only considered in the region $R = \sqrt{x^2 + y^2} \ll \epsilon$, $z \approx 0$ ($\eta \approx 0$) the finite coil looks like an infinite solenoid. In the plane $z = 0$

$$\begin{aligned} \mathbf{A}(\xi_R, 0, \varphi) &= A(R) \, \mathbf{n}_\varphi , \\ \mathbf{B}(\xi_R, 0, \varphi) &= B(R) \, \mathbf{n}_z , \end{aligned} \tag{10}$$

$$R = \epsilon\sqrt{\xi_R^2 - 1} = \epsilon \, P_1^1(\xi_R) . \tag{11}$$

Inside the coil $(R \le R_1)$

$$A(R) = \alpha R_1^{-2} \, R, \quad B(R) = 2\alpha R_1^{-2}, \tag{12}$$

while outside $(R \ge R_1)$

$$A(R) \sim \alpha \, R^{-1}, \quad B(R) \sim 0 . \tag{13}$$

Relations (13) are asymptotic series for $\epsilon \to \infty$, the omitted terms being of order $\epsilon^{-2}\ln(\epsilon^{-2})$. Figure 1 shows $A(R)$ and $B(R)$ for $\alpha = 1$, $R_1 = 1$, as a function of the eccentricity. It is seen that the vector potential of a coil with $L_1/R_1 \approx \epsilon = 30$ is, in the vicinity of its largest

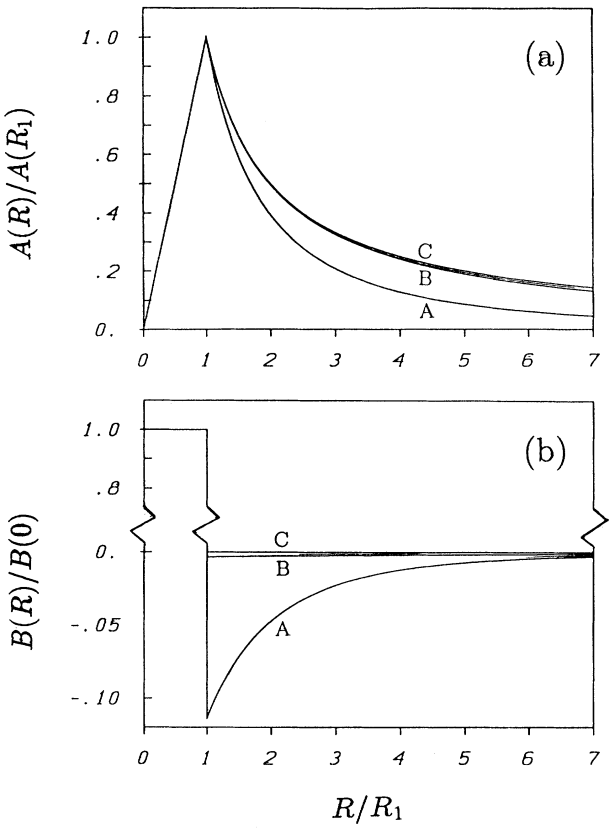

FIG. 1. (a) Scaled vector potential $A(R)/A(R_1)$ and (b) scaled magnetic field $B(R)/B(0)$ of a Maxwell coil (eccentricity ϵ, radius R_1) in the horizontal symmetry plane as a function of the scaled distance R/R_1. A, $\epsilon = 3$; B, $\epsilon = 30$; C, $\epsilon = \infty$.

diameter, essentially that of an infinite solenoid. The difference shows up only in the existence of a weak magnetic field outside the coil which exists in the whole plane $z = 0$ and compensates the flux inside the coil.

The return flux may be restricted to a finite domain if systems of two or more confocal coils are considered ($\epsilon = \epsilon_1 = \epsilon_2 = \cdots$, $R_1 < R_2 < \cdots$). In a system of two coils the currents (parameters $J_{1,2}$) may be determined as functions of the geometrical parameters ϵ, R_1, R_2 and the field inside the inner coil (parameter $\alpha = B R_1^2/2$).

$$B_1' + B_2' = 0, \quad B_1 + B_2 = B. \tag{14}$$

For this system the vector potential vanishes identically in the exterior of the larger coil and all flux lines close within this coil.

Likewise, in a three-coil system the vector potential vanishes outside the largest coil if the currents $J_{1,2,3}$ are determined from

$$B_1' + B_2' + B_3' = 0, \quad B_2 + B_3 = 0, \quad B_1 = B. \tag{15}$$

(B is the value of the field inside the central coil.) In the limit $\epsilon \to \infty$, $R_1 \to 0$, $R_2 \to R_3$, B fixed, this coil system approaches the string-plus-shell model considered in Refs. [7, 8].

III. THE THREE-DIMENSIONAL PROBLEM

A. Classical motion

To simplify formulas we consider a particle of unit mass and unit charge and use units where $c = 1$. Outside the (central) solenoid the classical motion of the particle is governed by the Hamiltonian

$$\begin{aligned} H &= \tfrac{1}{2}(\mathbf{p} - \mathbf{A})^2 \\ &= \frac{1}{2\epsilon^2(\xi^2 - \eta^2)}\left[p_\xi(\xi^2 - 1)p_\xi + p_\eta(1 - \eta^2)p_\eta\right] \\ &\quad + \frac{1}{2}\left[\frac{p_\varphi}{\epsilon\sqrt{(\xi^2 - 1)(1 - \eta^2)}} - A_\varphi(\xi, \eta)\right]^2, \end{aligned} \tag{16}$$

where, for a given coil system, the potential $A_\varphi(\xi, \eta)$ follows from (3). If more than one coil is present all but the smallest one are assumed to be penetrable. At the surface of this coil the particle is elastically reflected: when $\xi(t) = \xi_1$, p_ξ changes from $p_\xi(t)$ to $p_\xi(t + 0) = -p_\xi(t)$ while the momenta p_η and p_φ remain unchanged. From this reflection law and Hamilton's equations it follows that p_φ is a constant of motion.

Elimination of the momenta gives Newton's equations for the variables ξ, η, φ where the force is the Lorentz force due to the field (7) (and additional constant fields if more than one coil is present). Outside the (central) coil one therefore finds curved orbits which approach straight lines far away from the coil since the field decays rapidly for $r \to \infty$, or even vanishes for $r > r_{\max}$. We studied numerically these orbits for initial conditions $\mathbf{x}_0 = (x_0, y_0, z_0) = (-R_0, \delta_0 \cos\phi, \delta_0 \sin\phi)$ ($R_0 > 0$, $0 \le \phi \le 2\pi$), $\mathbf{v}_0 = (v_{x0}, v_{y0}, v_{z0}) = (K_0, 0, 0)$ ($K_0 > 0$), and calculated the deflection angles parallel to the plane $z = 0$ (angle Ω) and normal to it (angle ω). As the magnetic field of the back flux assumes its largest values near the surface of the central coil, the largest deflection angles were found for grazing rays. It turned out that $\omega_{\max}/\Omega_{\max} \approx \epsilon^{-1}$ for a single coil; for systems of two or three coils the ratio was even smaller since concentration of the back flux to a finite region results in larger z components of the field outside the central coil and hence larger angles Ω. In Sec. IV these results will be used to justify the approximation of the three-dimensional problem by a two-dimensional one.

B. Quantum mechanics

In units where $c = \hbar = 1$ the Hamilton operator $\hat{H}$ is obtained from the Hamiltonian H by the substitution

$$p_\xi \to -i\frac{\partial}{\partial\xi}, \quad p_\eta \to -i\frac{\partial}{\partial\eta}, \quad p_\varphi \to -i\frac{\partial}{\partial\varphi}, \tag{17}$$

where the sequence of factors in (16) has to be maintained. Since the (angular) momentum operator $\hat{p}_\varphi = -i\,\partial/\partial\varphi$ commutes with $\hat{H}$, the Hilbert space $\mathcal{H}$ may be decomposed into subspaces $\mathcal{H}_m$ which are invariant under the evolution. That is, if a wave function is decomposed according to

$$\psi(\xi,\eta,\varphi\,|\,t)=\sum_m \psi_m(\xi,\eta\,|\,t)\,e^{im\varphi}\,, \tag{18}$$

the functions ψ_m evolve according to the reduced Schrödinger equations

$$i\frac{\partial}{\partial t}\psi_m=\tfrac{1}{2}[\hat{T}+\hat{V}_m]\,\psi_m\,, \tag{19}$$

$$\hat{T}=-\frac{1}{\epsilon^2(\xi^2-\eta^2)}\left[\frac{\partial}{\partial\xi}(\xi^2-1)\frac{\partial}{\partial\xi}+\frac{\partial}{\partial\eta}(1-\eta^2)\frac{\partial}{\partial\eta}\right], \tag{20}$$

$$\hat{V}_m=\left[\frac{m}{\epsilon\sqrt{(\xi^2-1)(1-\eta^2)}}-A_\varphi(\xi,\eta)\right]^2. \tag{21}$$

Reflections at the hard spheroid $\xi=\xi_1$ are taken into account by the boundary condition

$$\psi_m(\xi_1,\eta\,|\,t)=0\,. \tag{22}$$

The components ψ_m of a square-integrable wave function $\psi\in\mathcal{H}$ satisfy

$$\int_{-1}^{1}\int_{\xi_1}^{\infty}|\psi_m(\xi,\eta\,|\,t)|^2\,\epsilon^3(\xi^2-\eta^2)\,d\xi d\eta<\infty \tag{23}$$

and (22), and each of these functions evolves according to Eqs. (19)–(21).

Therefore one is faced with two problems: First, the functions $\psi_m(\xi,\eta\,|\,0)$ have to be chosen in such a way that the total wave function $\psi(\xi,\eta,\varphi\,|\,0)$ represents an incoming wave packet. In principle, an infinite number of expectation values would be needed to fix this wave packet uniquely. However, only a few of them are relevant for the scattering process; these are especially the mean values and variances of position and velocity.

$$\langle\,\hat{\mathbf{x}}\,\rangle_{t=0}=\mathbf{x}_0,\qquad\langle\,\hat{\mathbf{p}}-\hat{\mathbf{A}}\,\rangle_{t=0}=\mathbf{v}_0, \tag{24}$$

$$\langle\,(\hat{\mathbf{x}}-\mathbf{x}_0)^2\,\rangle_{t=0}=\delta_0^2,\qquad\langle\,(\hat{\mathbf{p}}-\hat{\mathbf{A}}-\mathbf{v}_0)^2\,\rangle_{t=0}=\Delta_0^2. \tag{25}$$

The second problem that has to be mastered is the explicit solution of the initial-value problems for the components ψ_m. In Sec. IV we discuss an approximation in which the two-dimensional initial-value problems are replaced by one-dimensional ones, and present solutions of these simpler problems. At this point we only want to emphasize that Eqs. (19)–(22) describe the motion of a particle in a simply connected domain. For $\xi\to\infty$ free motion is approached because A_φ decays as ξ^{-2} (one coil) or vanishes for $\xi>\xi_{\max}$ (two- and three-coil systems). It is therefore obvious that standard quantization rules have to be applied and the eigenvalues m of the angular momentum $\hat{p}_\varphi$ have to be integers.

IV. THE TWO-DIMENSIONAL PROBLEM

A. The basic hypothesis

As already mentioned in Sec. III A classical scattering by Maxwell coils is essentially a two-dimensional problem if (i) the coil is very long, (ii) the particle starts from a position near the symmetry plane $z=0$ and moves parallel to it in the beginning, and (iii) the motion is only considered for times where $R(t)\ll\epsilon$. As in the region $|z|<\delta_0\ll\epsilon$, $R\ll\epsilon$, or

$$\xi^2-1\ll 1,\qquad|\eta|<\delta_0/\epsilon\qquad(\epsilon\gg 1)\,, \tag{26}$$

the field of the back flux is essentially parallel to the z axis and the reflecting surface of the coil nearly plane, the classical motion along the coordinate $z=\epsilon\xi\eta\approx\epsilon\eta$ may be neglected as long as one is only interested in motions confined to region (26). Formally this approximation is obtained by dropping the term $p_\eta(1-\eta^2)p_\eta$ in the Hamiltonian (16) and setting $\eta=0$ in the remaining terms. A classical distribution, initially centered around

$$\mathbf{x}_0=(-R_0,0,0),\qquad\mathbf{v}_0=(K_0,0,0) \tag{27}$$

$(R_0,K_0>0)$ would then, to a good approximation, evolve in time according to a Liouville equation derived from this simplified Hamiltonian.

It is known that for ordinary potential scattering there exist close analogies between classical distribution functions and their quantum equivalents (Wigner or Husimi functions). Especially for high momenta (short wavelengths) the latter are seen to differ from the former only inside the region of the geometrical shadow and near its boundaries. What is important here is that all the other regions, into which the classical distribution does not enter, are also never seen by the corresponding quantum distribution (in this argument tiny tails of distribution functions are neglected). We assume that this relation between classical and quantum distribution functions is also valid if magnetic interactions are included. If this is true, a wave packet starting with mean velocity $\mathbf{v}_0$ from $\mathbf{x}_0$ will remain in region (26) during the whole scattering process. For this restricted set of initial data it makes sense to simplify the three-dimensional quantum problem analogous to the classical one, i.e., to drop the term $\partial/\partial\eta\,(1-\eta^2)\,\partial/\partial\eta$ and to set $\eta=0$ in (19). As long as the wave function is considered only in domain (26), $\partial/\partial\xi=(\epsilon^2\xi/R)\partial/\partial R\approx(\epsilon^2/R)\partial/\partial R$ so that the evolution equation for the function $\psi_m(\xi_R,0\,|\,t)=\Psi_m(R\,|\,t)$ becomes

$$i\frac{\partial}{\partial t}\Psi_m=\tfrac{1}{2}\left[\hat{T}+\hat{V}_m\right]\Psi_m\,, \tag{28}$$

$$\hat{T}=-\frac{1}{R}\frac{\partial}{\partial R}R\frac{\partial}{\partial R}\,, \tag{29}$$

$$\hat{V}_m=\left[\frac{m}{R}-A(R)\right]^2. \tag{30}$$

The boundary condition reads

$$\Psi_m(R_1)=0 \tag{31}$$

and the normalization condition becomes, in this approximation,

$$\int_{R_1}^{\infty}|\Psi_m(R\,|\,t)|^2\,R\,dR=c_m<\infty\,. \tag{32}$$

Equations (28)–(31) comprise all two-dimensional AB scattering problems for which analytical stationary solutions have been found in the past. What is new here is that we are looking for square-integrable solutions (wave packets), and that the potential $A(R)$ is due to one or several coils of finite length. Moreover, we believe that the solutions of Eqs. (28)–(31), multiplied with a Gaussian in the variable η, constitute an approximate solution of the three-dimensional initial-value problem given by (19)–(22). In Sec. V we extend the conclusions drawn from the solutions of the two-dimensional problem to the still idealized but more realistic three-dimensional problem. As the following steps are straightforward and can be checked by standard methods, the only way to prove that our conclusions are irrelevant for the three-dimensional problem would consist in solving explicitly Eqs. (19)–(21) for appropriate initial data.

B. Initial data

In the reduced initial-value problem the wave function at $t = 0$ is assumed to be a two-dimensional Gaussian wave packet.

$$\Psi(\mathbf{X}\,|\,0) = \mathcal{N}\, e^{-\gamma(\mathbf{X}-\mathbf{X}_0)^2 + i\mathbf{K}_0\cdot(\mathbf{X}-\mathbf{X}_0)}. \tag{33}$$

In (33) $\mathbf{X} = (x, y) = (R\cos\varphi, R\sin\varphi)$ is the space variable, $\mathcal{N} = \sqrt{2\gamma/\pi}$ a normalization constant, and

$$\mathbf{X}_0 = (-R_0, 0), \quad \mathbf{K}_0 = (K_0, k_0). \tag{34}$$

The constant k_0 is chosen such that the kinetic angular momentum vanishes at $t = 0$.

$$\langle \hat{p}_\varphi + \hat{R}A(\hat{R})\rangle_{t=0} = 0. \tag{35}$$

For the Gaussian (33) the first term of (35) is equal to $(\mathbf{X}_0 \times \mathbf{K}_0)_z$; hence

$$k_0 = -\langle \hat{R}A(\hat{R})\rangle_{t=0}/R_0\ . \tag{36}$$

The mean position at $t = 0$ is then $-R_0\,\mathbf{n}_x$ and the x component of the velocity is $\langle \hat{P}_x - \hat{A}_x\rangle_{t=0} = K_0$. If $2\delta_0 = \gamma^{-1/2} \ll R_0$ the y component becomes vanishingly small. The boundary condition (31) is satisfied numerically if $R_0 - \delta_0 \gg R_1$.

At $t = 0$ the components in the decomposition

$$\Psi(R, \varphi\,|\,t) = \sum_m \Psi_m(R\,|\,t)\, e^{im\varphi} \tag{37}$$

are obtained by means of the formula

$$e^{i(u\cos\phi + v\sin\phi)} = \sum_m \left(\frac{iu+v}{\sqrt{u^2+v^2}}\right)^m J_m(\sqrt{u^2+v^2})\, e^{im\phi} \tag{38}$$

which is also valid for complex parameters u, v.

$$\begin{aligned}\Psi_m(R\,|\,0) &= \mathcal{N}\, e^{-\gamma(R^2+R_0^2+iK_0R_0)} \left(\frac{a}{b}\right)^m J_m(bR),\\ a &= k_0 - 2\gamma R_0 + iK_0,\\ b &= \left(K_0^2 + k_0^2 - 4\gamma^2 R_0^2 + 4i\gamma K_0 R_0\right)^{1/2}.\end{aligned} \tag{39}$$

From the properties of the Bessel functions J_m [15] it may be deduced that

$$\Psi_m \approx 0 \quad \text{for} \quad |m| > M = K_0/\sqrt{\gamma} \tag{40}$$

in the beginning ($t = 0$). Because of (32) the magnitude of these components cannot increase in time so that only $2M + 1$ components have to be taken into account if the wave packet is initially of the form (33).

C. Numerical integration

The evolution in time of the components Ψ_m is calculated numerically. We employ a scheme which was apparently first used by Goldberg and Schey [16] for one-dimensional problems and applied later by Gailbraith, Ching, and Abraham [17] to two-dimensional scattering problems (see also [18]). In this approach, a variant of the so-called "operator-splitting" method, the evolution operator for a time interval of length 2τ is factorized according to

$$\begin{aligned}\hat{U}_m(2\tau) &= \exp\left[-i\tau\left(\hat{T} + \hat{V}_m\right)\right]\\ &\to \hat{W}_m(\tau)\hat{Q}(2\tau)\hat{W}_m(\tau)\ .\end{aligned} \tag{41}$$

In (41) the "potential propagator"

$$\hat{W}_m(\tau) = \exp(-i\tau\hat{V}_m/2) \tag{42}$$

is a multiplicative operator, and the "kinetic propagator" $\hat{Q}(2\tau)$ is approximated by its Cayley form,

$$\hat{Q}(2\tau) = \exp(-i\tau\hat{T}) \to \frac{\hat{1} - i(\tau/2)\hat{T}}{\hat{1} + i(\tau/2)\hat{T}}. \tag{43}$$

The operators $\hat{T}$ and $\hat{V}_m$ are given by (29) and (30), respectively. That the n-fold product of operators of the form (41) with $2\tau = t/n$ tends to $\hat{U}(t)$ for $n \to \infty$ follows from Trotter's formula. If the equation $\hat{U}_m(2\tau)\,\Psi_m(R\,|\,t_j) = \Psi_m(R\,|\,t_{j+1})$ is multiplied with $[\,\hat{1} + i(\tau/2)\hat{T}\,]\,\hat{W}(-\tau)$ one obtains

$$\begin{aligned}&[\,\hat{1} - i(\tau/2)\hat{T}\,]\,\hat{W}(\tau)\ \Psi_m(R\,|\,t_j)\\ &\qquad = [\,\hat{1} + i(\tau/2)\hat{T}\,]\,\hat{W}(-\tau)\ \Psi_m(R\,|\,t_{j+1})\ .\end{aligned} \tag{44}$$

The algorithm based on (44) is stable for arbitrary time steps 2τ [18].

Numerical treatment of (44) requires also discretization of the space variable, $R_\ell = \ell\rho$,

$$\Psi(R_\ell\,|\,t_j) \to \Psi(\ell\,|\,j)\ , \tag{45}$$

and the differential operator (29) has to be replaced by a difference operator.

$$\hat{T}\,\Psi(R\,|\,t)\Big|_{R=R_\ell,t=t_j} \to \frac{1}{\rho^2}\left[-\left(1+\frac{\rho}{2R_\ell}\right)\Psi(\ell+1\,|\,j)+2\Psi(\ell\,|\,j)-\left(1-\frac{\rho}{2R_\ell}\right)\Psi(\ell-1\,|\,j)\right]. \tag{46}$$

In order to obtain $\Psi_m(\ell'\,|\,j+1)$ from $\Psi_m(\ell\,|\,j)$ the evolution equation (44) has to be supplemented with the boundary conditions

$$\Psi_m(\ell_{\min}\,|\,j)=\Psi_m(\ell_{\max}\,|\,j)=0\,. \tag{47}$$

The first of these conditions is nothing but (31), the boundary condition at the surface of the (central) coil ($R_1=\ell_{\min}\rho$). The second condition follows from (32); it replaces the natural boundary conditions for the square-integrable components [$\Psi_m(R\,|\,t)\to 0$ for $R\to\infty$]. In every time step the calculation of the numbers $\Psi_m(\ell\,|\,j)$ can be drastically reduced since the tails of the wave packet Ψ and all its components Ψ_m can be neglected outside an interval of the form $\ell(j)\le\ell\le\ell(j)+L$. In our calculations the length L of this interval was chosen such that the values of $|\Psi|^2$ at the corners were smaller than the maximum value within the interval by a factor 10^{-6} or more. The boundaries $\ell(j)$ and $\ell(j)+L$ were adjusted after each time step in accordance with the motion of the peak of $|\Psi_0|^2$. To check the accuracy of the scheme the norm of the wave packet was calculated repeatedly in each time run.

The algorithm outlined above was tested for two limits where the solution of the initial-value problem can be given in closed form (free motion, constant magnetic field). For time steps of magnitude $2\tau=10^{-4}$ agreement between analytical and numerical wave functions was found to be excellent for $\rho=0.0025$ and satisfactory for $\rho=0.01$.

D. Results

The evolution of wave packets was followed for more than 3×10^3 time steps. Initially the wave packets were centered on the negative x axis, the distance to the center of the coil(s) being $R_0=3$ (Figs. 2 and 3) or $R_0=5$ (Figs. 4 and 5). At $t=0$ the width of the packet was given by the parameter $\gamma=1.535\,057$, or $2\delta_0=1/\sqrt{\gamma}\approx0.8$ [cf. (25) and (33)]. As can be seen from Figs. 2–5 the radial width of the packet after the scattering is of the same order of magnitude, i.e., the asymptotic evolution, where the packet spreads linearly in time in radial direction, is not included in our calculations. In most cases the initial velocity was chosen to be $K_0=30$, but lower ($K_0=10$) and larger values ($K_0=120$) were also considered in order to verify the correct behavior for long and short wavelengths. The number of components considered for $K_0=30$ was 95; when the components with $|m|>47$ are removed, the norm of Ψ, originally equal to 1, is only reduced by an amount of order 10^{-4}.

The radius of the inpenetrable coil was chosen to be $R_1=0.2$; the radii of other coils are $R_2=2.5$ in the two-coil system, and $R_2=2.0$, $R_3=2.5$ in the three-coil system. The eccentricities varied between $\epsilon=7$ (Figs. 3 and 4) and $\epsilon=\infty$ (infinite solenoid, Figs. 2 and 5).

Figures 2–5 show snapshots of $|\Psi|^2$ (contour lines) at selected instants. Initially the packet moves upwards; after the scattering it moves away in all directions. However, in the scale used here, the intensity of the scattered packet is too small to be visible outside a certain neighborhood of the forward direction. A finer scale would also show a flat peak which originates from the reflection at the inpenetrable coil and moves essentially backwards. This scale was not used in the drawings since this effect is well understood and would only obscure the essential message of our figures.

Figure 2(a) shows the scattering of a wave packet by an inpenetrable cylinder ($\alpha=0$, cf. [17]). The originally bell-shaped probability distribution evolves to a butterflylike form when the wave packet "hits" the cylinder. The superposition of incoming and outgoing parts of the packet results in a wavy structure where the distance between adjacent crests is determined by the momentum K_0. The highest crest is the one which encloses the obstacle in U form; the vanishing intensity between its two legs marks the region of geometrical shadow. As time proceeds, the parts of the butterflylike figure move more and more outwards in radial direction, but an azimuthal motion persists also for some time. Especially the two ends of the main crest get into contact at a finite distance behind the cylinder, and the two branches of the wave packet start to interfere constructively. Finally, the azimuthal motion comes practically to an end and the resulting distribution, a central peak with two symmetric side maxima, moves radially outwards with velocity K_0; during this motion the radial profile of the distribution spreads. At large distances from the cylinder, and outside

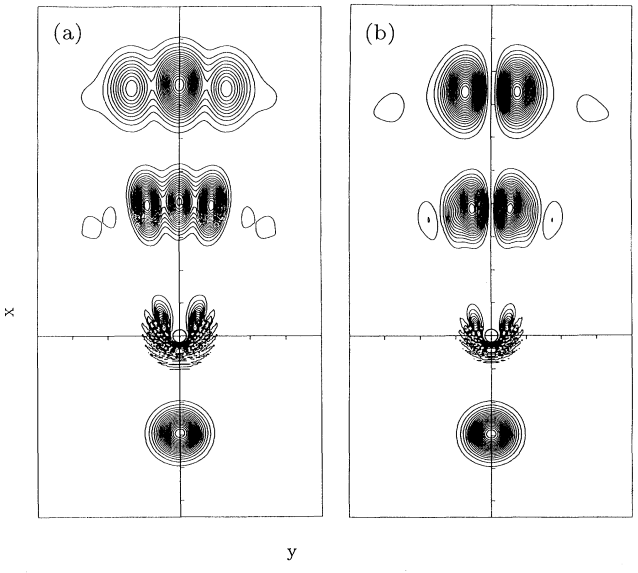

FIG. 2. Scattering of a wave packet by an inpenetrable infinite solenoid ($\epsilon=\infty$): Contour lines of $|\psi|^2$ at subsequent instants (from bottom to top: $t=0.00$, 0.12, 0.24, 0.36). Flux parameters: (a) $\alpha=0.0$, (b) $\alpha=0.5$.

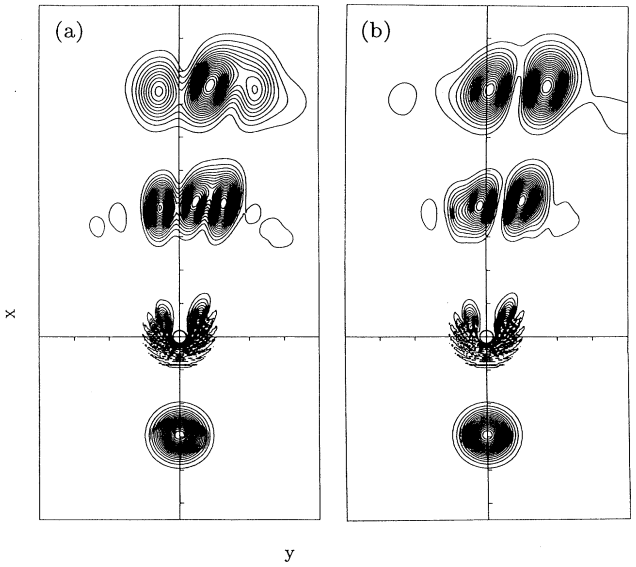

FIG. 3. Scattering of a wave packet by an inpenetrable Maxwell coil ($\epsilon = 7$): Contour lines of $|\psi|^2$ at subsequent instants (from bottom to top: $t = 0.00,\ 0.12,\ 0.24,\ 0.36$). Flux parameters: (a) $\alpha = 10.0$, (b) $\alpha = 10.5$.

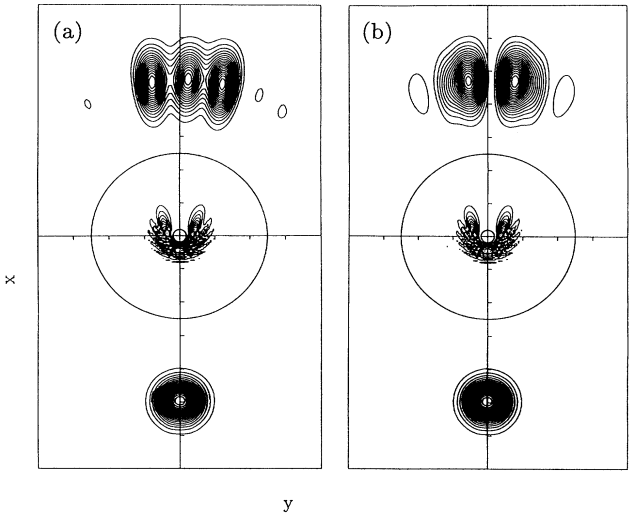

FIG. 4. Scattering of a wave packet by an inpenetrable Maxwell coil enclosed by a penetrable one which contains the magnetic back flux ($\epsilon_1 = \epsilon_2 = 7$): Contour lines of $|\psi|^2$ at subsequent instants (from bottom to top: $t = 0.00,\ 0.18,\ 0.33$). Flux parameters: (a) $\alpha = 10.0$, (b) $\alpha = 10.5$.

a narrow sector containing the central peak, the angular distribution of the outgoing wave packet becomes proportional to the differential cross section obtained from time-independent scattering theory [19, 11].

Except for minor modifications the first part of this evolution is also seen in all other figures. In Fig. 2(b) the infinite solenoid encloses a magnetic field with flux parameter $\alpha = 0.5$. Scattering by the hard core of the coil proceeds as for $\alpha = 0$ and the region of geometrical shadow is the same. However, when the two wings of the butterfly unite behind the coil these parts of the wave packet interfere destructively: instead of the central peak a minimum of vanishing intensity, sandwiched by two maxima of equal height, appears behind the obstacle. This agrees qualitatively with the conclusions AB derived from time-independent scattering theory [1]. This theory predicts vanishing of the total wave function at large distances behind the solenoid (here the positive x axis), but yields also arbitrarily large values of the scattering amplitude in the vicinity of this direction. However, this divergence of the differential cross section in forward direction and the resulting divergence of the total scattering cross section should not be taken literally; they result only from applying the statistical interpretation of quantum mechanics to non-normalizable stationary solutions of the Schrödinger equation. In a proper time-dependent treatment, where only square-integrable wave functions are considered, these difficulties do not occur at all. Figure 2(b) shows that the divergences at both sides of the forward direction are reduced to two peaks of finite height. This smoothing of the divergent scattering amplitude may be attributed to the fact that an infinite number of stationary eigenfunctions with slightly differing wave vectors has to be superposed in order to obtain a wave packet of finite norm.

We note in passing that for the cylindrical solenoid ($\epsilon = \infty$) the relation between the asymptotic forms of the incoming and the outgoing wave packet (theoretically $t \to \mp\infty$; here $t < 0.00$ and $t > 0.36$, respectively) can also be obtained by analytic methods [11]. These calculations show that the double peak found for $\alpha = 0.5$ evolves

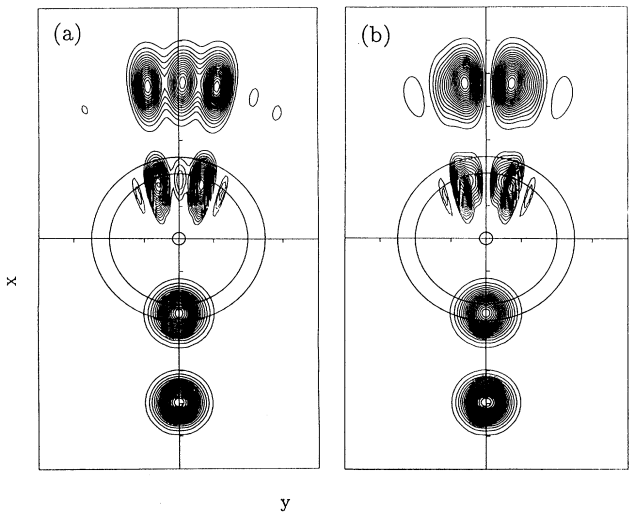

FIG. 5. Scattering of a wave packet by an inpenetrable infinite solenoid enclosed by a cylindrical shell which contains the magnetic back flux ($\epsilon_1 = \epsilon_2 = \epsilon_3 = \infty$): Contour lines of $|\psi|^2$ at subsequent instants (from bottom to top: $t = 0.00,\ 0.09,\ 0.23,\ 0.33$). Flux parameters: (a) $\alpha = 1.0$, (b) $\alpha = 0.5$.

gradually from the central peak and one of its neighbors [cf. Fig. 2(a)] as α is increased from zero to 0.5 (the other side maximum degenerates to a small hump). Although this asymptotic analysis is very useful for discussing the physical meaning of cross sections and the optical theorem, it contains much less information on the scattering process than the explicit solution of the time-dependent Schrödinger equation presented in Fig. 2. Only this full description of the evolution allows one to differentiate between hard-core scattering ($t \approx 0.12$), which is essentially independent of the field inside the solenoid, and the AB interference pattern that emerges subsequently behind the geometrical shadow of the coil and depends crucially on the enclosed magnetic flux.

The other figures illustrate the influence of the magnetic back flux. In Fig. 3 the magnetic field is that of a Maxwell coil with $\epsilon = 7$. Because of the weak magnetic field outside the coil, the wave packet, which starts moving in the x direction, is slightly deflected and the "collision" with the coil is no longer central; this can be seen from the asymmetry of the butterfly. The packet feels the magnetic field also after the scattering by the hard coil, but becomes a free packet in the end since the field decays rapidly. Compared to the asymptotic angular distribution obtained for the infinite coil, the number of the peaks is the same and they are of the same magnitude. But the whole pattern is now shifted as one would expect from the action of the Lorentz force. The same effect is seen for the two-coil system in Fig. 4 ($\epsilon = 7$) where the back flux is restricted to the interior of the larger coil.

Finally, in Fig. 5 the back flux of the central solenoid ($\epsilon = \infty$) is confined to a cylindrical shell; no magnetic field exists in the region between the solenoid and the shell and outside the shell. In Refs. [7, 8] this situation was discussed in terms of time-independent scattering theory, and it was concluded that the scattering amplitude of this problem is due to the Lorentz force from the magnetic field in the shell. Figure 5 disproves this conjecture: transition through the shell, both before and after the scattering by the central coil, results only in small distortions of the wave packet. As in the other examples the characteristic AB interference pattern evolves when the two wings of the butterfly, which are of nearly the same magnitude but have in general different phases, approach each other behind the inpenetrable coil. The result of this interference, e.g., the difference between $\alpha = 0$ and $\alpha = 0.5$, is already clearly visible before the packet passes the shell for the second time. That is, six different stages of the evolution are clearly perceivable in this example: (1) free motion of the Gaussian wave packet; (2) transition of this packet through the magnetic shell—a minor effect; (3) hard-core scattering by the central solenoid—essentially independent of the enclosed flux (not shown in Fig. 5); (4) flux-dependent AB interference behind the shadow region; (5) transition of the wave packet carrying the characterisitic AB interference pattern through the magnetic shell—again a minor effect; and (6) free outgoing radial motion outside the shell, including spreading in this direction. Since the field inside the shell decreases with increasing diameter, if the flux of the central coil is kept constant, it is obvious that the influence of the shell becomes negligible as its radius tends to infinity. It is therefore not surprising that also in a time-independent approach the results of AB are regained when the diameter of the shell tends to infinity [7, 8]. However, this fact does not indicate that the magnetic AB effect is caused by the Lorentz force of the back flux. On the contrary, this and the previous examples (Figs. 3 and 4) show unequivocally that the formation of the AB interference pattern and the deflection due to magnetic fields outside the coil which splits the incoming beam are independent effects. This is in agreement with Kobe's results for the two-slit experiment [9]: When an extended magnetic field is added to the shielded coil behind the screen, the interference pattern due to the two slits and the trapped flux persists, but is now shifted in accordance with the classical Lorentz force acting on the electron.

V. CONCLUSION

In this paper the magnetic Aharonov-Bohm (AB) effect is reconsidered. In their pioneering work [1] AB considered the scattering of electrons by a solenoid of infinite length and vanishing diameter. This thought experiment, as well as its modifications proposed by other authors subsequently, were discussed in terms of time-independent scattering theory (for exceptions see [12, 3]) and the geometry was restricted to two space dimensions. It is obvious that an infinite solenoid may be viewed as a limit of finite ones. In Sec. II we recall that there exist coils of prolate sheroidal shape, which produce constant fields in their interior and for which both vector potential and magnetic field can be given in closed analytical form. For these coils, called Maxwell coils in the literature, we then formulate in Sec. III the three-dimensional scattering problem as an initial-value problem for square-integrable wave functions (wave packets). In this problem the space accessible to the particle is simply connected and the motion approaches a free motion at large distances from the coil. It is therefore clear that the usual quantization conditions have to be employed; they result in integer eigenvalues of the angular momentum component along the coil's axis.

From the study of the classical orbits we conclude that the three-dimensional problem may be approximated by a two-dimensional one if (i) the coil is very long; (ii) the particle starts from a position near the symmetry plane normal to the axis and moves parallel to it in the beginning; and (iii) the motion is followed only as long as the distance between particle and coil is much smaller than the length of the coil. It should be possible to verify or to disprove this hypothesis by more extensive numerical calculations. We are not only confident that such a calculation will corroborate the results of our two-dimensional approximation, which is derived in Sec. IV by heuristic arguments, but we also want to point out that the solution of the three-dimensional problem would allow one to pass continuously from an apparently two-dimensional problem to a truly three-dimensional one. Scattering off the top of a slim Maxwell coil should constitute a mathe-

matical model of scattering by a tapered iron whisker for which the AB effect has been observed experimentally [2]. If this expectation can be verified by numerical calculations it would be obvious that the only purpose of impenetrable obstacles, may they be of finite or infinite extension, is to split the wave packet, or part of it, and to keep the parts separated by a shadow region which contains a magnetic flux. To discuss the topological properties of the space in which the particle could move *in principle*, but does not under the given (initial) conditions, and to consider related modifications of quantization conditions would then turn out to be a mere mathematical exercise which is irrelevant for physical experiments.

The numerical solutions of the two-dimensional problems presented in Sec. IV lead to the following picture of three-dimensional AB scattering: In the beginning, when the wave packet is scattered by the hard core of the coil, the evolution in time is independent of the enclosed magnetic flux. The hard coil determines the gross features of the angular distribution of the outgoing packet, especially outside the forward direction, and serves to slit the packet in forward direction. At finite distance behind the coil the two parts of the packet, which passed the coil on different sides, unite again and their relative phases become important. These phases vary with the current in the coil in the way predicted by AB so that the enclosed flux, or the vector potential outside the coil, becomes visible in the form of the interference pattern behind the hard coil. Although the details of the angular distribution depend on the instant of observation, its qualitative features, i.e., the number of the peaks and their symmetry, are already visible at this time. Magnetic fields outside the inpenetrable coil, may they be due to the finite length of the coil and/or additional penetrable coils enclosing the central one, result only in an additional deflection of the packet which corresponds to the deflection of classical particles by the Lorentz force.

ACKNOWLEDGMENT

This research was supported by the Austrian Science Foundation (FWF) under Project No. P7888.

[1] Y. Aharonov and D. Bohm, Phys. Rev. **115**, 485 (1959).
[2] M. Peshkin and A. Tomura, *The Aharonov-Bohm Effect* (Springer, Berlin, 1989).
[3] S. Olariu and I. I. Popescu, Rev. Mod. Phys. **57**, 339 (1985).
[4] S. M. Roy, Phys. Rev. Lett. **44**, 111 (1980); U. Klein, Phys. Rev. D **23**, 1463 (1981); H. J. Lipkin, *ibid.* **23**, 1466 (1981).
[5] M. Peshkin, I. Talmi, and L. J. Tassie, Ann. Phys. (NY) **12**, 426 (1961).
[6] L. J. Tassie, Phys. Lett. **5**, 43 (1963).
[7] J. Q. Liang, Phys. Rev. D **32**, 1014 (1985).
[8] D. H. Kobe and J. Q. Liang, Phys. Rev. A **37**, 1133 (1988).
[9] D. H. Kobe, Ann. Phys. (NY) **123**, 381 (1979).
[10] M. Babiker and R. Loudon, J. Phys. A **17**, 2973 (1984).
[11] M. Jursa and P. Kasperkovitz, J. Phys. A (to be published).
[12] M. Kretzschmar, Z. Phys. **185**, 84 (1965).
[13] P. M. Morse and H. Feshbach, *Methods of Theoretical Physics* (McGraw-Hill, New York, 1953).
[14] J. Meixner and F. W. Schäfke, *Mathieusche Funktionen und Sphäroidfunktionen* (Springer, Berlin, 1954).
[15] M. Abramowitz and I. E. Stegun, *Handbook of Mathematical Functions* (Dover, New York, 1965).
[16] H. Goldberg and H. M. Schey, Am. J. Phys. **35**, 177 (1967).
[17] I. Gailbraith, Y. S. Ching, and E. Abraham, Am. J. Phys. **52**, 60 (1984).
[18] W. H. Press, B. P. Flannery, S. A. Teukolsky, and W. T. Vetterling, *Numerical Recipes* (Cambridge University Press, Cambridge, 1986).
[19] W. O. Amrein, J. M. Jauch, and K. B. Sinha, *Scattering Theory in Quantum Mechanics* (Benjamin, Reading, MA, 1977).